

# Redundant and Distinct Functions for Dynamin-1 and Dynamin-2 Isoforms

Yoram Altschuler,<sup>‡</sup> Shana M. Barbas,<sup>\*</sup> Laura J. Terlecky,<sup>\*</sup> Kitty Tang,<sup>‡</sup> Stephen Hardy,<sup>§</sup> Keith E. Mostov,<sup>‡</sup> and Sandra L. Schmid<sup>\*</sup>

<sup>\*</sup>Department of Cell Biology, The Scripps Research Institute, La Jolla, California 92037; <sup>‡</sup>Department of Anatomy, University of California, San Francisco, California 94143; and <sup>§</sup>Cell Genesys Inc., Foster City, California 94404

**Abstract.** A role for dynamin in clathrin-mediated endocytosis is now well established. However, mammals express three closely related, tissue-specific dynamin isoforms, each with multiple splice variants. Thus, an important question is whether these isoforms and splice variants function in vesicle formation from distinct intracellular organelles. There are conflicting data as to a role for dynamin-2 in vesicle budding from the TGN. To resolve this issue, we compared the effects of overexpression of dominant-negative mutants of dynamin-1 (the neuronal isoform) and dynamin-2 (the ubiquitously expressed isoform) on endocytic and biosynthetic membrane trafficking in HeLa cells and polarized MDCK cells. Both dyn1(K44A) and dyn2(K44A) were potent inhibitors of receptor-mediated endocytosis;

however neither mutant directly affected other membrane trafficking events, including transport mediated by four distinct classes of vesicles budding from the TGN. Dyn2(K44A) more potently inhibited receptor-mediated endocytosis than dyn1(K44A) in HeLa cells and at the basolateral surface of MDCK cells. In contrast, dyn1(K44A) more potently inhibited endocytosis at the apical surface of MDCK cells. The two dynamin isoforms have redundant functions in endocytic vesicle formation, but can be targeted to and function differentially at subdomains of the plasma membrane.

**Key words:** receptor-mediated endocytosis • dynamin • polarized MDCK cells • *trans*-Golgi network • adenovirus expression

**T**HE GTPase dynamin is required for late stages in endocytic clathrin-coated vesicle formation. Dynamin is targeted to coated pits on the plasma membrane, in a guanine nucleotide-independent manner (44), through interactions between its proline, arginine rich COOH-terminal domain (PRD) and the SH3-domain containing protein, amphiphysin (16, 36). Amphiphysin binds, through other regions of the molecule, to both  $\alpha$ -adaptin and clathrin (12, 32, 56, 60). Initially, dynamin is uniformly distributed throughout the clathrin lattice (10, 59), but subsequent GTP binding triggers its self-assembly into a helical collar encircling the necks of deeply invaginated pits (50). It has been suggested that coordinated GTP hydrolysis by the assembled dynamin molecules results in a concerted conformational change and generates a force necessary, but not sufficient, to detach the coated vesicle from the plasma membrane (20, 57).

Many aspects of this model must be tested and the exact

role of dynamin in coated vesicle formation remains unknown (39). However, in support of this model, it has recently been shown that purified dynamin can assemble cooperatively and in a nucleotide-independent manner around acidic liposomes to form long tubules (49). Strikingly, addition of GTP, but not nonhydrolyzable analogues, caused rapid fragmentation of these dynamin-encircled tubules.

*Drosophila* and *Caenorhabditis elegans* appear to express only a single isoform of dynamin (7, 8, 54), mutations in which perturb synaptic vesicle recycling in neurons and bulk phase endocytosis in all tissues examined (26, 27). In contrast, mammals exhibit tissue-specific expression of three closely related (>80% identical) dynamin isoforms: dynamin-1 (dyn1)<sup>1</sup> is exclusively expressed in neurons, dynamin-2 (dyn2) is ubiquitously expressed, and dynamin-3 (dyn3) is expressed in testes and to a lesser extent in neurons and lung (for review see reference 53). Moreover, each isoform has multiple splice variants, leading to the

Address correspondence to Sandra L. Schmid, Department of Cell Biology, The Scripps Research Institute, 10550 N. Torrey Pines Rd., IMM11, La Jolla, CA, 92037. Tel.: (619) 784-2311. Fax: (619) 784-9426. E-mail: slschmid@scripps.edu

1. *Abbreviations used in this paper:* B-Tfn, biotinylated-transferrin; dyn1, dynamin-1; dyn2, dynamin-2; GFP, green fluorescent protein; MPR, cation-independent mannose-6-phosphate receptor; Tfn, transferrin.

suggestion that the different isoforms and splice variants of dynamin might participate in vesicular trafficking events at distinct intracellular locations (53). This model is attractive in that it infers that the machinery used for vesicle budding from one organelle could be targeted for use at multiple sites in the cell, in analogy to the involvement of rab-family GTPases along distinct trafficking pathways. In support of this model, GFP-fusion proteins generated with different isoforms and splice variants of dynamin were differentially localized when expressed in clone 9 cells (6). Most striking was the differential distribution of dyn2(aa) and dyn2(ab) isoforms that differ only by a 4-amino acid insert: the latter was exclusively localized to plasma membrane-associated coated pits, whereas the former was associated with clathrin-coated buds at both the plasma membrane and TGN. Finally, evidence has been presented that dyn2 is required in a cell-free system for the formation of both constitutive and clathrin-coated vesicles from the TGN (22).

Functional studies *in vivo* have thus far failed to provide evidence for dyn2-function at the TGN. Inducible overexpression of dominant-negative mutants of dyn1 in stably transformed HeLa cells potently inhibited endogenous dyn2 function in clathrin-mediated endocytosis but did not affect biosynthetic trafficking through the Golgi to either the plasma membrane or to lysosomes (9). Moreover, endogenous dyn2 was exclusively localized to clathrin-coated pits at the plasma membrane (9) in these cells. These results suggested that both dyn1 and dyn2 function exclusively in clathrin-mediated endocytosis. More recent studies in endothelial or epithelial cells indicate that the internalization of caveolae is also dynamin dependent (18, 35).

In an effort to identify a possible role for dyn2 at the TGN and to resolve these conflicting results we have reexamined the specificity of dynamin function by comparing the effects of dyn1(K44A) and dyn2(K44A) dominant-negative mutants on membrane trafficking in HeLa cells and in polarized MDCK cells.

## Materials and Methods

### Cells and Antibodies

HeLa cells stably expressing the tetracycline-regulatable chimeric transcription activator (tTA-HeLa) were obtained from H. Bujard (Zentrum Für Molekular Biologic, Heidelberg, Germany; 15) and cultured as previously described (9). tTA-MDCK cells were as previously described (1). This cell line is now available from CLONTECH Laboratories, Inc. (Palo Alto, CA). Antibodies used in this study were: mouse anti-dynamin monoclonal antibody (hudy-1) that recognizes a shared epitope between dyn1 and dyn2 (9, 58); goat anti-mannose-6-phosphate receptor antibody (obtained from K. von Figura, University of Göttingen, Göttingen, Germany); rabbit anti-mannose-6-phosphate receptor antibody (obtained from B. Hoflack, Institute de Biologie de Lille, Lille, France); rabbit anti-cathepsin D antibodies (obtained from W. Brown and K. von Figura); mouse anti- $\gamma$ -adaplin antibody, 100/3 (Sigma Chemical Co., St. Louis, MO); rabbit anti- $\gamma$ -adaplin antibody (obtained from M.S. Robinson, University of Cambridge, Cambridge, UK); rabbit anti-clathrin light chain antibody (obtained from E. Ungewickell, Washington University, St. Louis, MO); rabbit anti-TGN48 antibody (obtained from S. Ponnambalan, University of Dundee, Dundee, UK); mouse anti-human transferrin receptor (TfnR) antibodies, B3/125 and D65 (obtained from I. Trowbridge, Salk Institute, La Jolla, CA); and sheep anti-SC antibody recognizing the extracellular domain of pIgR (1). Rat antibody (3F10) against the HA epitope was obtained from Boehringer Mannheim Corp. (Indianapolis, IN). Hybridoma

cells secreting mouse anti-E-cadherin mAb (rr1; Gumbiner and Simmons, 1986), which recognizes the extracellular epitope were a gift from B. Gumbiner (Sloan Kettering, New York, NY). Mouse mAb supernatant against gp135, a MDCK apical membrane glycoprotein (Ojakian and Schwimmer, 1988) was provided by G. Ojakian (SUNY Health Science Center, Brooklyn, NY).

### Construction of Recombinant Adenoviruses

The tetracycline regulated promoter followed by coding sequences for either the wild type or dominant negative K44A mutant of dynamin-1 (aa splice variant) or dynamin-2 (ba splice variant) were subcloned from the tetracycline inducible expression plasmid pUHD10-3 to pAdlox (17) 3' to the  $\psi$ 5 packaging site and 5' to the polyA site, replacing the original CMV promoter with the regulated tetracycline promoter. Viruses were produced as described in detail elsewhere (17).

### Viral Infection and Overexpression of wt and Mutant Dynamin

tTA-HeLa cells ( $2.5 \times 10^6$ ) were seeded on 10-cm dishes for 3–5 h. Media was removed and the cells were incubated with 3  $\mu$ l of dyn1(wt) virus stock or 0.3  $\mu$ l of dyn1(K44A), dyn2(wt), or dyn2(K44A) virus stock, corresponding to ~15 plaque-forming units/cell of recombinant adenoviruses in 2 ml of binding media (Hank's salts containing 1 mM MgCl<sub>2</sub>, 1 mM CaCl<sub>2</sub>, and 10 mM Hepes, pH 7.2) for 2 h at 37°C to enable viral attachment and infection. Binding media was removed and cells were incubated for 18 h in culture media. Overexpression levels relative to endogenous dynamin were determined by Western blotting of known numbers of cell equivalents using the pan-dynamin antibody 748 (55). Specifically, the intensity of the dynamin band in a standard curve generated by loading  $10^3$ – $5 \times 10^4$  infected cells was determined using ECL detection and a scanning densitometer and compared with that in a standard curve corresponding to  $5 \times 10^4$ – $2 \times 10^5$  uninfected cells. The amount of each virus stock used for infection was empirically determined by titrating virus and assessing cell morphology and dynamin expression (using phase contrast and immunofluorescence microscopy). The amount of virus used corresponded to that which gave no adverse effects on cell morphology whereas producing dynamin expression in ~90% of the cell population.

MDCK T23 cells (4) were seeded at confluency 4 d before the assay on 12-mm Transwell™ (Costar Corp., Cambridge, MA). 18 h before the assay, cells were infected for 2 h with 2  $\mu$ l of dyn1(wt) virus stock or 0.14  $\mu$ l of dyn1(K44A), dyn2(wt), or dyn2(K44A) per Transwell™ corresponding to ~40 plaque-forming units/cell in PBS lacking CaCl<sub>2</sub>. Then monolayers were washed twice with MEM media containing Earle's balanced salt solution (Cellgro; Mediatech, Inc., Washington, DC) supplemented with 5% FBS (Hyclone, Logan, UT) 100 U/ml penicillin, 100  $\mu$ g/ml streptomycin, in 5% CO<sub>2</sub>/95% air at 37°C. Cells were further incubated for 18 h to express the indicated recombinant proteins.

### Membrane Trafficking Assays

Assays for Tfn endocytosis, Tfn recycling, TfnR biosynthesis and trafficking through the Golgi to the plasma membrane, cathepsin D biosynthesis and trafficking to the lysosome, and fluid phase endocytosis of HRP were performed in tTA-HeLa cells as previously described (9). Assays for Tfn endocytosis, pIgR endocytosis, and polarized TGN to cell surface targeting of pIgR in MDCK cells were performed as previously described (2).

Recycling of IgA was performed as follows: MDCK T23 cells were incubated with MEM plus 0.6% BSA and 20 mM Hepes (pH 7.4) at 4°C and allowed to bind <sup>125</sup>I-IgA for 60 min at the apical surface. Unbound ligand was removed by extensive washing over a period of 45 min with medium at 4°C. Cells were then rapidly warmed to 37°C for 5 min and immediately cooled back to 4°C. IgA at the apical surface was removed by two sequential incubations of 10 min each in cold media containing 25  $\mu$ g/ml trypsin. Cells were then washed three times over a period of 30 min with cold media. Cells were warmed up to 37°C for the indicated times in the presence of 25  $\mu$ g/ml trypsin at the apical media to prevent reinternalization of the ligand. IgA at the apical surface was removed by a 1-h treatment of 0.15 M glycine, pH 2.5, in PBS. At the end of the assay the basolateral media, stripped cells on filters, apical media, and material stripped from the apical surface were harvested and radioactivity was quantitated in a Packard gamma counter. Recycled IgA was calculated as the amount of stripped IgA from the apical surface plus the IgA secreted into the apical media divided by the total IgA internalized.

## Immunofluorescence

tTA-HeLa cells were grown on coverslips and infected with recombinant adenoviruses as described above. Before fixation for immunofluorescence, virally infected cells were permeabilized with streptolysin O (SLO) to remove the soluble pool of overexpressed dynamin. Thus, cells were incubated with streptolysin O (5  $\mu$ g/ml in PBS) for 3 min on ice, washed with PBS<sup>++</sup> and incubated with 3 min at 37°C in the presence of KSHM buffer (100 mM KOAc; 85 mM sucrose; 25 mM Hepes, pH 7.2; 1 mM MgOAc) to generate pores in the plasma membrane. Cells were then returned to ice and incubated for 5 min in fresh KSHM to allow diffusion of cytosolic contents, before fixation in 3.5% PFA in PBS<sup>++</sup>. Cells were then permeabilized with PBS<sup>++</sup> containing 0.05% saponin and 4% goat serum. Antibody incubations were performed at room temperature in permeabilization buffer. Secondary antibodies used were: Alexa488-goat anti-mouse and Texas red goat anti-rabbit (Molecular Probes, Inc., Eugene, OR) or FITC mouse anti-rabbit and Texas red mouse anti-goat (Jackson Labs). Coverslips were mounted using Aquamount (Polysciences, Inc.) and visualized using a Zeiss Axiovert 100TV, with the Bio-Rad MRC1024 confocal system at 63 $\times$ .

For basolateral surface labeling, MDCK T23 cells were incubated for 60 min at 4°C with the monoclonal antibody rr1 that recognizes the extracellular domain of native E-cadherin. Unbound antibody was removed by extensive washing over 30 min at 4°C before fixation of the cells with 4% paraformaldehyde. Cells were permeabilized with 0.025% (wt/vol) saponin in PBS and blocked with 20 mM glycine. This was followed by sequential incubations with the remaining primary antibodies followed by goat anti-mouse Alexa494 and goat anti-rat Alexa488-conjugated secondary antibodies (minimum cross reactivity). The samples were analyzed using a BioRad MRC-1024 confocal microscope equipped with a krypton-argon laser and an Optiphot II Nikon microscope with a Plan Apo 60 $\times$  1.4 NA objective lens.

## Results

### Tetracycline Regulatable Expression of dyn1 and dyn2 Using Recombinant Adenoviruses

To facilitate analysis of dynamin function in multiple cell types, we generated recombinant adenoviruses encoding wild-type and K44A mutant dyn1(aa) and dyn2(ba). This splice variant of dyn2 has been reported to localize to both the TGN and plasma membrane when expressed as a GFP-fusion protein (5). As the toxicity of overexpression of these proteins might have affected the packaging efficiency and production of recombinant viruses, the cDNAs were placed under control of a tetracycline-regulatable promoter. Also, to increase production efficiency and yield of recombinant virus we used the Cre-Lox system for adenoviral production (17). In this way, high titer preparations of recombinant virus were routinely obtained (see Materials and Methods). Conditions for viral infection were determined that resulted in nearly 100% infection efficiency (as judged by immunofluorescence), optimal expression of dynamin (assessed by Western blotting) and minimal toxic effects on cells (assessed by cell morphology). Minimizing cell toxicity was especially important for maintaining cell polarity and monolayer resistance when infecting MDCK cells.

When HeLa cells stably expressing a chimeric tetracycline-regulatable transcription activator (tTA-HeLa) were infected with recombinant adenovirus, expression of recombinant dynamins was strictly dependent on the concentration of tetracycline in the media. In the absence of tetracycline, dyn1(K44A) and dyn2(K44A) mutants were expressed at >200 and >50-fold over endogenous dyn2, respectively. Addition of tetracycline to the media suppressed dynamin expression in a concentration dependent

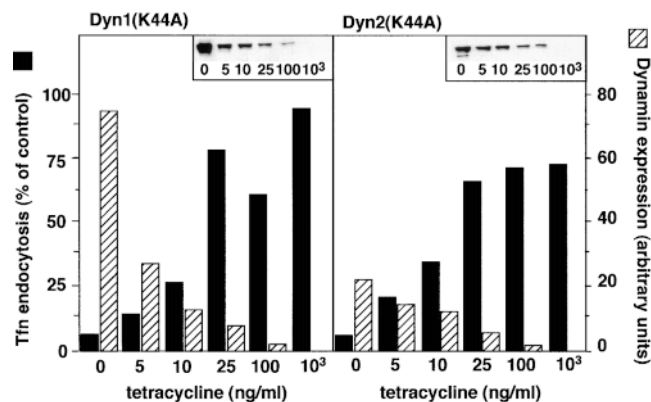


Figure 1. Tetracycline-regulatable expression of dynamin mutants in adenovirally infected tTA-HeLa cells. tTA-HeLa cells were infected with recombinant adenovirus encoding mutant dyn1 and dyn2 under control of a tetracycline (tet)-regulatable promoter. After infection, cells were incubated for 16–18 h in the presence of the indicated concentrations of tet. Tfn endocytosis was measured as indicated in Materials and Methods and is shown by the solid bars relative to uninfected control cells. Inserts show Western blots of dynamin expression that was quantitated by ECL detection and scanning densitometry and shown by the hatched bars.

manner (Fig. 1). To determine the relative potency of the two dynamin isoform mutants, endocytosis assays were performed after expression in the presence of increasing concentrations of tetracycline; an example of which is shown in Fig. 1. Based on three such experiments, we concluded that maximum inhibition of endocytosis required >40-fold excess dyn1(K44A) and >10-fold excess dyn2 (K44A).

To avoid potential nonspecific effects of very high levels of overexpression, all further experiments were performed in the presence of 5 ng/ml tetracycline, unless otherwise specified. Under these conditions, dyn1(K44A) and dyn2 (K44A) were expressed at ~60- and ~20-fold over endogenous dyn2, respectively, and both mutants potently inhibited the rate and extent of receptor-mediated endocytosis (Fig. 2, filled symbols). In contrast, overexpression of wt dyn1 or dyn2 had no effect (Fig. 2, open symbols), even at the high levels of overexpression achieved in the absence of tetracycline (not shown).

### Endosomal Recycling Is Unaffected by Overexpression of dyn2(K44A)

As expected, overexpression of mutant dyn1 and dyn2 molecules led to an increase in the cell surface expression of TfnR (not shown). This suggested that neither isoform functions in receptor recycling from the endosome. However, given that clathrin-coated vesicles appear to bud from endosomes and have been proposed to play a role in membrane recycling (48), we directly examined the effects of the dynamin mutants on the rates and extents of TfnR recycling. For these experiments, cells were incubated for 60 min in the presence of saturating concentrations of B-Tfn to load the recycling endosomal compartments to steady state. Surface bound Tfn was masked by addition of

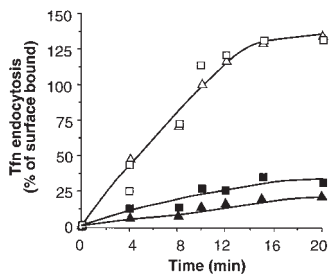


**Figure 2.** Tfn endocytosis is potently inhibited by dyn1 (K44A) and dyn2(K44A). tTA-HeLa cells were infected with recombinant adenovirus encoding dyn1(wt) (□), dyn2(wt) (Δ), dyn1 (K44A) (■), or dyn2(K44A) (▲). Cells were incubated in the presence of 5 ng/ml tet for 18 h to induce expression.

Tfn endocytosis was measured by incubating cells with 4 μg/ml B-Tfn for the indicated times as 37°C before measuring intracellular B-Tfn based on its inaccessibility to avidin as previously described (55). Results shown are expressed as the percentage internalized at 37°C vs. total bound at 4°C and are >100% owing to internalization of recycled Tfn-receptors. They are representative of >5 experiments.

avidin at 4°C and the cells were reincubated at 37°C in the presence of avidin to mask cell associated B-Tfn as it reappears on the cell surface. The data in Fig. 3 A shows that neither dyn1(K44A) nor dyn2(K44A) mutants significantly affected the recycling of TfnR from endosomes to the plasma membrane. Similarly, the efficient recycling of IgA internalized from and recycled back to the apical surface was unaffected by overexpression of wt or mutant dyn1 or dyn2 in MDCK cells (Fig. 3 B). A small fraction (<10%) of IgA internalized at the apical surface is delivered to the basolateral surface. Neither the rate nor the extent of this transcytotic pathway was affected by overexpression of dyn1(K44A) or dyn2(K44A) (data not shown).

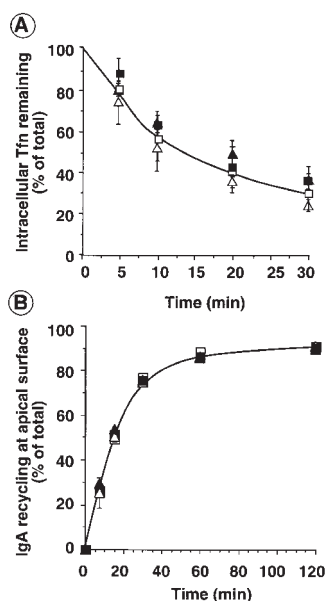


**Figure 3.** Recycling from endosomes is unaffected by dyn1(K44A) or dyn2(K44A). Adenovirally infected tTA-HeLa cells (A) or MDCK T23 cells (B) overexpressing dyn1(wt) (□); dyn1(K44A) (■); dyn2(wt) (Δ), or dyn2 (K44A) (▲) were cultured for 18 h after infection in the presence (A) or absence (B) of 5 ng/ml tet. (A) HeLa cells were then loaded with B-Tfn at 37°C to steady state. Surface bound B-Tfn was masked with avidin at 4°C and the recycling of intracellular B-Tfn was determined after incubation at 37°C for the indicated times as described in Materials and Methods. (B) MDCK T23 cells were incubated with <sup>125</sup>I-IgA at 4°C for 60 min and unbound IgA was eliminated by three quick washes with cold media. Surface bound ligand was internalized by warming the cells to 37°C for 5 min. Cells were then cooled down, cell surface IgA was removed by trypsin treatment, and the recycling of intracellular <sup>125</sup>I-IgA was determined, as described in Materials and Methods, after incubation at 37°C for the indicated times. Results shown are average of three experiments.

### Fluid-Phase Endocytosis Continues in Cells Overexpressing dyn2(K44A)

It had previously been shown that endocytosis of fluid phase markers continues in cells overexpressing dominant-negative mutants of dyn1 (9, 10, 19, 30). Similarly, blocking the recruitment of endogenous dyn2 to coated pits by overexpression of the SH3 domain of amphiphysin inhibited TfnR and EGFR endocytosis but did not block fluid phase uptake (61). In contrast, fluid phase endocytosis is blocked in *Drosophila* cells carrying mutations in the dynamin homologue, *shibire* (24, 25) suggesting that the ubiquitously expressed dynamin might be required for this process. However, we found that fluid phase endocytosis continues in HeLa cells expressing dyn2(K44A) at the same rate as that seen in cells expressing wt dyn2 or in uninfected cells (Fig. 4). These data confirm previous findings that fluid-phase endocytosis in mammalian cells can proceed in a dynamin-independent manner.

### Vesicular Trafficking at the TGN Is Unaffected by Overexpression of dyn2(K44A) Mutants

We next examined the effect of overexpression of the dyn2(K44A) mutants on trafficking through the Golgi apparatus. As was reported for stable cell lines induced to overexpress dyn1(K44A), the rate and extent of transport of newly synthesized TfnR from the ER through early Golgi compartments as assessed by acquisition of EndoH resistance was unaffected by overexpression of dyn2 (K44A) mutant (data not shown). Similarly, the rates of delivery of newly synthesized TfnR to the plasma membrane in cells expressing dyn2(K44A) mutant were indistinguishable from cells overexpressing dyn1(K44A) (Fig. 5 a). In both cases, however, we detected a slight delay relative to cells overexpressing either wt dynamin isoform. We also examined the transport of newly synthesized proteins to both the basolateral and apical surfaces on polarized MDCK cells. As can be seen in Fig. 5 b, the efficiency of polarized sorting of newly synthesized polymeric Ig receptor to the basolateral plasma membrane domain was unaffected in MDCK cells expressing either dyn1(K44A) or dyn2(K44A). These data suggest that the formation of three distinct classes of constitutive transport vesicles from the TGN is insensitive to disruption by dominant-negative mutants of dyn2.

To determine whether dyn2 functions in clathrin-mediated vesicle budding from the TGN we examined the effects of dynamin mutant overexpression on the rate and

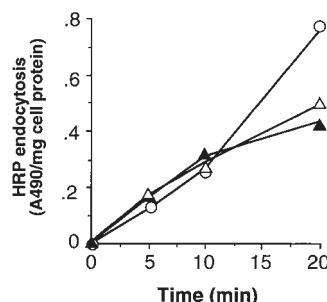


**Figure 4.** Initial rates of fluid phase endocytosis are unaffected by overexpression of dyn2(K44A). Endocytosis of HRP into noninfected cells (○) or adenovirally infected tTA-HeLa cells expressing either wt (Δ) or K44A (▲) dyn2 was assessed as described in Materials and Methods. Results shown are representative of >4 experiments.

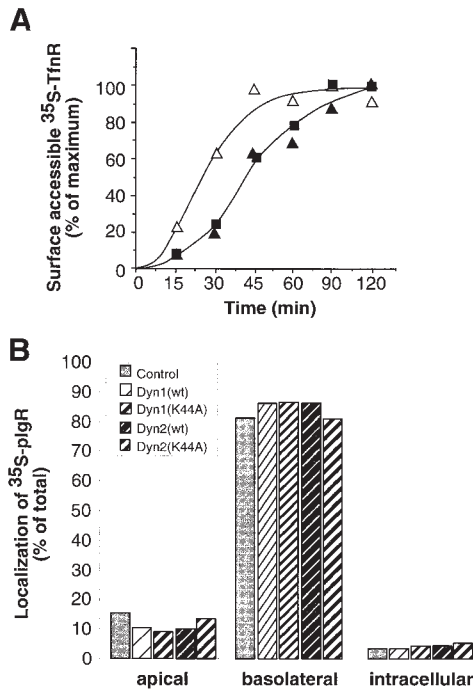


**Figure 5.** Delivery of three classes of biosynthetic transport vesicles from the TGN to the plasma membrane in cells overexpressing dyn1 and dyn2 mutants. (A) Adenovirally infected tTA HeLa cells overexpressing dyn2(wt) ( $\Delta$ ), dyn2(K44A) ( $\blacktriangle$ ), or dyn1(K44A) ( $\blacksquare$ ) were pulse-labeled with  $^{35}\text{S}$ -translabel for 30 min at  $37^\circ\text{C}$  and then incubated in methionine-containing chase media for the indicated times. The appearance of newly synthesized TfnR on the cell surface was determined by its susceptibility to trypsin digestion as described in Materials and Methods. The results shown are representative of three experiments. (B) Adenovirally infected MDCK T23 cells or uninfected control cells were pulse-labeled for 10 min with  $^{35}\text{S}$ -methionine followed by incubation at  $37^\circ\text{C}$  in chase media. The distribution of biosynthetically labeled pIgR was determined following immunoprecipitation of intracellular or apical or basolateral membrane associated pools as previously described (2).

extent of cathepsin D transport from the TGN to lysosomes. Cathepsin D is a 49-kD mannose-6-phosphate-containing lysosomal hydrolase that under normal conditions binds to the mannose-6-phosphate receptor (MPR) in the TGN and is transported to the endosomal compartment via clathrin-coated vesicles (13a). Upon encountering lysosomal processing enzymes it is cleaved to the 32-kD mature form. As shown in Fig. 6, the rates of cathepsin D processing in cells overexpressing dyn2(K44A) were indistinguishable from those expressing dyn1(K44A). Again, cells overexpressing mutant dynamin isoforms exhibited a slight retardation in the rates of cathepsin D processing. We also examined the extent of secretion of newly synthesized cathepsin D into the media to determine whether the sorting efficiency for lysosomal hydrolases was affected by overexpression of dyn2(K44A). These assays were performed in the presence of 5 mM mannose-6-phosphate to prevent binding to surface expressed MPR and possible reuptake. In three experiments,  $9.6 \pm 2\%$  of newly synthesized cathepsin D was secreted in cells expressing dyn2(wt)

compared with  $8.6 \pm 1.6\%$  and  $8.4 \pm 0.7\%$  in cells expressing dyn1(K44A) or dyn2(K44A), respectively. Furthermore, there was no detectable change in the rate of cathepsin D secretion in wt or mutant cells (not shown). Thus, overexpression of dyn2(K44A) had little effect on the sorting or trafficking of the lysosomal enzyme cathepsin D from the TGN in HeLa cells.

### Overexpression of dyn2(K44A) Does Not Affect the Steady State Distribution of TGN48 or MPR

Our studies suggest that dyn2 function is not required for the formation of at least four classes of transport vesicles from the TGN, including: apically and basolaterally directed biosynthetic transport vesicles in polarized MDCK cells, and plasma membrane and lysosomally directed biosynthetic transport vesicles in nonpolarized cells. However, we have previously shown that cells expressing a temperature-sensitive mutant of dynamin, dyn1(G273D), rapidly respond to inhibition of clathrin-mediated endocytosis by induction of a clathrin-independent pathway for endocytic vesicle formation (11). Similarly, vacuolar sorting of lysosomal hydrolases is inhibited at early time points after shift to the nonpermissive temperature in yeast expressing a temperature-sensitive mutant of clathrin, but quickly recovers so that at later time points the transport of lysosomal hydrolases is unaffected (42). Therefore, it remained possible that the cells had compensated by induction of a new pathway for plasma membrane or lysosomal trafficking during the several hours they experience overexpression of mutant dyn2(K44A). Such an induction might account for the slight delay in the kinetics of these transport events observed in cells expressing mutant dyn1 and dyn2.

We therefore sought other evidence for this apparent specificity of dynamin function by examining the localiza-

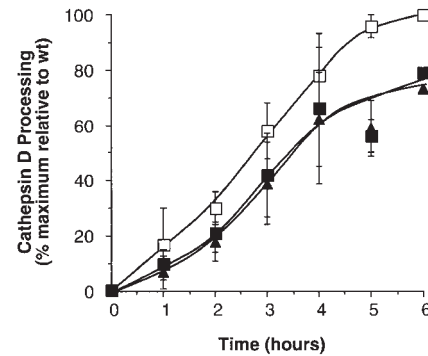


**Figure 6.** Cathepsin D processing is not significantly inhibited in cells overexpressing dyn1 or dyn2 mutants. Adenovirally infected tTA HeLa cells overexpressing dyn1(wt) ( $\square$ ), dyn1(K44A) ( $\blacksquare$ ), or dyn2(K44A) ( $\blacktriangle$ ) were pulse-labeled with  $^{35}\text{S}$ -translabel for 30 min at  $37^\circ\text{C}$  and then incubated in methionine-containing chase media for the indicated times. The appearance of the mature form of cathepsin D in late endosomes/lysosomes was determined following immunoprecipitation and quantitation using PhosphorImager analysis as described in Materials and Methods. The results are expressed as percent of wt control and are the average of three experiments.

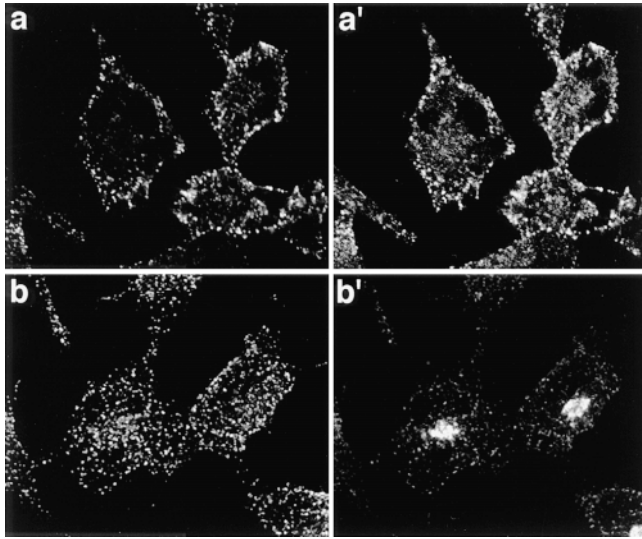


**Figure 7.** Immunofluorescence localization of endogenous dyn2 in HeLa cells. tTA-HeLa cells were processed for indirect immunofluorescence as described in Materials and Methods. Shown is the punctate localization of endogenous dyn2, as detected using the mAb Hudy-1 (*a* and *b*), its colocalization with puncta located at the cell periphery detected using anti-clathrin light chain rabbit sera (*a'*) and the lack of colocalization with the human TGN48, detected using monospecific rabbit sera (*b'*). Secondary antibodies were Alexa 488-conjugated goat anti-mouse and Texas red-conjugated goat anti-rabbit. Images were obtained using a Zeiss Axiovert 100TV, with the Bio-Rad MRC1024 confocal system and show a projection of either 4 optical sections taken through the middle of the cell (*a* and *a'*) or of 12 optical sections from the bottom to top of the cell (*b* and *b'*).

tion of endogenous and overexpressed wt and mutant dyn2 relative to known markers of the TGN and of TGN-derived transport vesicles. Endogenous dyn2 shows a punctate staining pattern uniformly distributed throughout the cell periphery (Fig. 7, *a* and *b*). At the cell periphery, these puncta overlap substantially with clathrin-coated pits, as detected using an affinity purified polyclonal antibody to clathrin light chains (Fig. 7 *a'*). In contrast, we were unable to detect any colocalization of endogenous dyn2 with the TGN marker, TGN48 (Fig. 7, *b* and *b'*).

The localization of endogenous dyn2 in HeLa cells is consistent with the localization of the dyn2(ab) isoform expressed in clone 9 cells (6). We therefore compared the localization of endogenous dyn2 with overexpressed wt and mutant dyn2(ba) isoform. Whereas wt dyn2 might transiently associate with a target membrane during vesicle detachment, we would anticipate that dyn2(K44A) might remain on its target membrane, trapped in the process of vesicle detachment. As seen in Fig. 8, exogenously expressed wt and K44A mutant dyn2 both showed a punctate staining pattern, similar to that seen for endogenous dyn2, that significantly overlapped with clathrin staining at the plasma membrane (Fig. 8, *b* and *c*). As with endogenous dyn2, we were unable to detect overlap with the clathrin label in the perinuclear region of the cell, nor could we detect colocalization with either TGN-associated AP1 adaptors (Fig. 8, *d-f*) or with TGN48 (Fig. 8, *g-i*) in HeLa cells.

For these images, cells were permeabilized with SLO before fixation to remove the excess soluble pool of dynamin and confocal optical sections were taken so that the localization of membrane associated dyn2 was not obscured by the overabundant soluble pool.

Previous studies on fibroblasts from I-cell patients defective in the tagging of lysosomal hydrolases with M6P-containing oligosaccharides, established that cathepsin D could by-pass the MPR pathway and be transported to lysosomes in vesicles devoid of MPR (14). However, trafficking of the MPR itself from the TGN appears to require the clathrin-coated vesicle machinery (28, 31). Thus, if dyn2(K44A) mutants inhibited-coated vesicle formation at the TGN then we should alter the steady state distribution of the MPR from the late endosomal compartment to the TGN. This expected redistribution occurs in cells overexpressing dominant-negative clathrin hub mutants (29). The micrographs in Fig. 8 show that the distribution of MPR relative to AP1 adaptors (Fig. 8, *g* and *h*) or TGN48 (Fig. 8, *i* and *j*) was indistinguishable in cells overexpressing dyn2(K44A) (Fig. 8, *h* and *j*) from those overexpressing dyn2(wt) (Fig. 8, *g* and *i*). These localization studies support our suggestion that the function of dynamin-2 in membrane trafficking is restricted to the plasma membrane.

#### *Differential Effects of dyn1 and dyn2 Mutants on Endocytosis in Polarized MDCK Cells*

Although overexpression of dominant-negative mutants of dyn1 and dyn2 had indistinguishable effects on membrane trafficking in HeLa cells, we found striking differences in the ability of dyn1(K44A) and dyn2(K44A) to inhibit endocytosis at the different plasma membrane domains in polarized MDCK cells. The data in Fig. 9 *a* shows that overexpression of dyn2(K44A) inhibited receptor mediated endocytosis of both TfnR (gray bars) and pIgR (hatched bars) at the basolateral surface in polarized MDCK cells. Endocytosis of pIgR was less affected by dyn2(K44A) perhaps reflecting differences in the relative efficiencies of endocytosis through clathrin-coated pits. In contrast, at these levels of overexpression, dyn1(K44A) mutants had no effect on endocytosis of either TfnR or pIgR from the basolateral surface (Fig. 9 *a*). The extent of inhibition of Tfn endocytosis at the basolateral surface (~70–80%) was less than that obtained in HeLa cells (~90%) perhaps because the levels of overexpression (~10-fold over endogenous dyn2) were lower than that obtained in tTA-HeLa cells. Several factors contribute to these lower levels of expression: first, infection is performed at a lower multiplicity of infection to ensure stability of the MDCK cell monolayer; second, the endogenous levels of dyn2 expression are higher in MDCK cells than in HeLa cells (unpublished data); and third, the expression level of the tTA transcription factor likely differs between the two transformed cell lines. Thus, in polarized MDCK cells, dyn2(K44A) appears to be a much more potent inhibitor of receptor-mediated endocytosis at the basolateral surface than dyn1(K44A).

Strikingly, the opposite was true for endocytosis at the apical surface. Because TfnRs are delivered preferentially to the basolateral surface, pIgRs are the best marker for

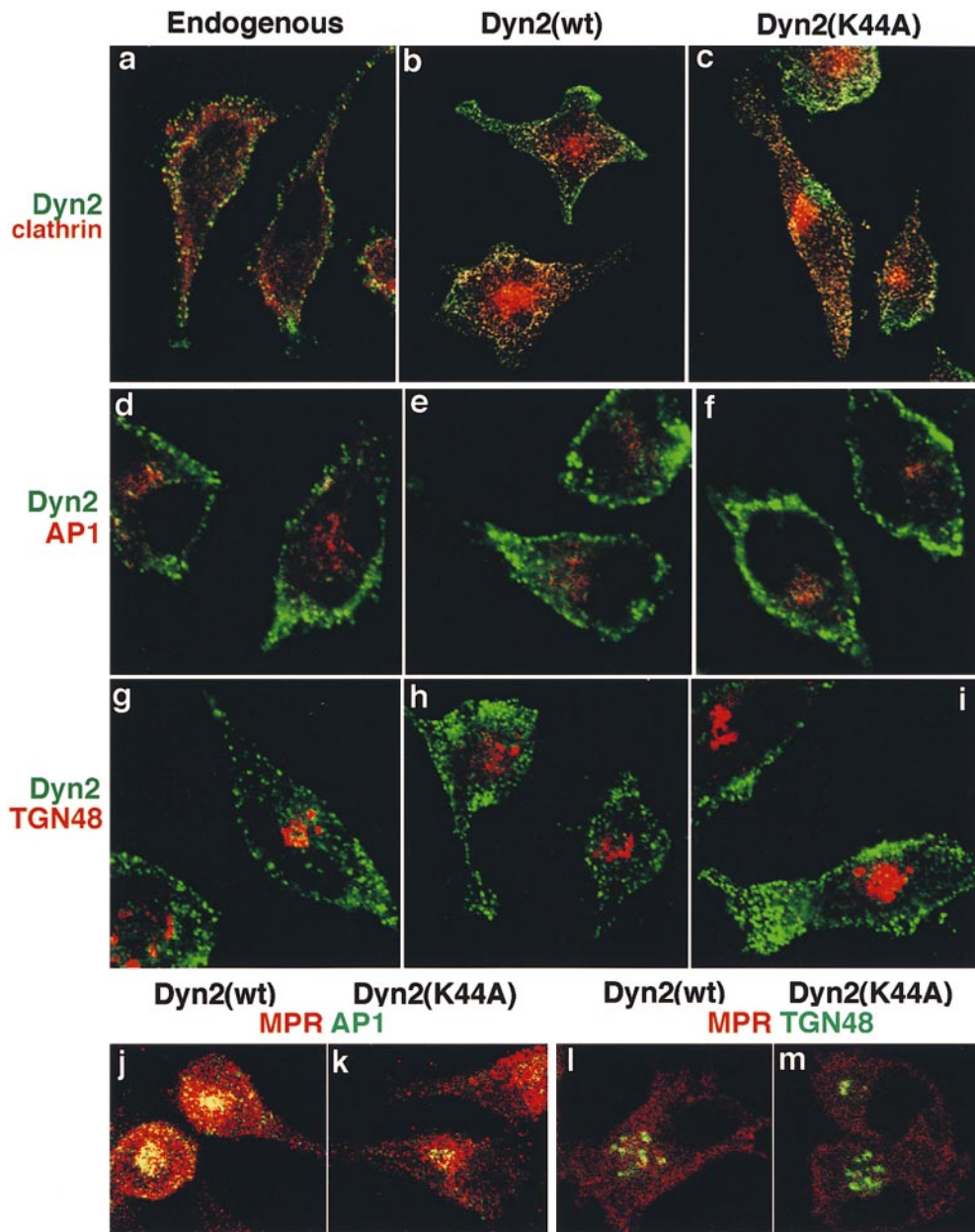


**Figure 8.** Immunofluorescence localization of endogenous and overexpressed dyn2 in HeLa cells. Uninfected tTA-HeLa cells (*a*, *d*, and *g*) or adenovirally infected tTA-HeLa cells expressing dyn2(wt) (*b*, *e*, *h*, *j*, and *l*) or dyn2(K44A) (*c*, *f*, *i*, *k*, and *m*) were fixed with 4% PFA and processed for indirect immunofluorescence as described in Materials and Methods. For dynamin localization in adenovirally infected cells overexpressing recombinant dynamin, cells were permeabilized with streptolysin O and cytosol was removed before fixation (*b*, *c*, *e*, *f*, *h*, and *i*). Primary antibodies used are indicated on the figure and their sources are given in Materials and Methods. Dyn2 = mAb anti-dynamin antibody, hudy1; clathrin = rabbit polyclonal anti-clathrin light chain; AP1 = rabbit polyclonal anti- $\gamma$  adaptin; TGN48 = rabbit polyclonal anti-human TGN48; MPR = rabbit polyclonal anti-MPR (*j* and *k*) or goat polyclonal anti-MPR (*l* and *m*). Images were obtained using a Zeiss Axiovert 100TV, with the Bio-Rad MRC1024 confocal system and show sections through the top (*a*–*c*) or middle (*d*–*k*) of the cell.

endocytosis at the apical surface. As can be seen, overexpression of dyn1(K44A) potently (= 80%) inhibited pIgR internalization from the apical plasma membrane (Fig. 9 *b*). At these levels of overexpression, the effects of dyn1(K44A) on pIgR endocytosis at the apical surface were more pronounced than those of dyn2(K44A) which inhibited pIgR uptake equally well (~40–50% inhibition) at both surfaces. Thus, in nonpolarized cells or at the basolateral surface of polarized MDCK cells, dyn2(K44A) appears to be a more potent inhibitor of clathrin-mediated endocytosis; whereas, at the apical surface of polarized MDCK cells, dyn1(K44A) appears to be more potent.

These data suggest that dyn1 is more efficiently targeted to the apical surface than it is to the basolateral surface. This speculation was confirmed by examining the distribution of dyn1 and dyn2 relative to apical or basolateral

plasma membrane markers in polarized MDCK cells. Fig. 10 *A* shows confocal sections through the apical surface of MDCK cells expressing either dyn1(K44A) or dyn2(K44A). The cells were costained with the apical plasma membrane marker, gp135. Dyn1(K44A) overlaps extensively with the gp135, as shown by the significant amount of yellow color in the merged image. Consistent with the functional data, dyn2(K44A) can also be detected at the apical surface but, as indicated by the much smaller amount of yellow color in the merged image, is present at lower levels relative to dyn1. Note that the apical surface has a characteristically speckled appearance, due to microvilli.

The opposite situation was observed when a confocal section through the basolateral region of the cell was taken, at the level of the nucleus (Fig. 10 *B*). In this case, E-cadherin was used as a marker of the lateral plasma

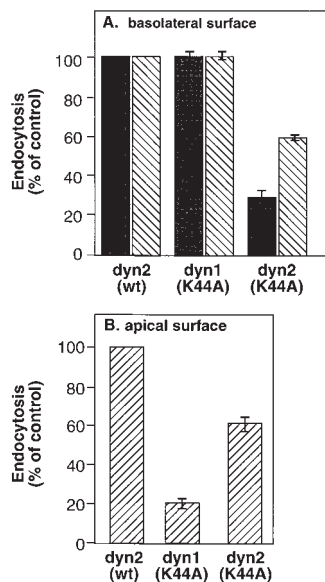


**Figure 9.** Differential effects of dyn1(K44A) and dyn2(K44A) on endocytosis in polarized MDCK cells. MDCK T23 cells were infected with recombinant adenovirus encoding either dyn2(wt), dyn1(K44A) or dyn2(K44A) and further incubated for 18 h at 37°C. Endocytosis from the basolateral (A) or apical surface (B) was determined by incubating cells for 1 h at 4°C in the presence of <sup>125</sup>I-Tfn (solid bars) or <sup>125</sup>I-IgA (striped bars) as described in Materials and Methods. Cells were next washed to remove unbound ligand and then rapidly warmed to 37°C for 5 min. Surface associated ligands were stripped by extensive washing with 0.15 M glycine in PBS. The extent of internalization relative to noninfected control cells is shown.

extensive washing with 0.15 M glycine in PBS. The extent of internalization relative to noninfected control cells is shown.

membrane. With dyn1(K44A), most of the signal was cytoplasmic and did not overlap extensively with E-cadherin, as shown by the absence of yellow color in the merged image. In striking contrast, dyn2(K44A) was largely localized to the lateral surface and overlapped with E-cadherin, resulting in very significant yellow color in the merged image. Note that with increasing levels of overexpression, we observe increased cytoplasmic staining, but not increased membrane association of dynamin (not shown), suggesting that once the membrane is saturated, excess dynamin becomes cytoplasmic, but does not seem to associate with the incorrect plasma membrane surface. Together, these data suggest that the two dynamin isoforms are preferentially targeted to and function at distinct domains of the plasma membrane.

### Discussion

A role for dynamin in clathrin-mediated endocytosis is now well-established (41, 57). New evidence indicates that both dynamin isoforms can also mediate the detachment of caveolae from the plasma membrane in endothelial and epithelial cells (18, 35). In addition to these shared functions, a specific role for dyn2 in vesicle budding from the TGN has also been proposed (22). However, overexpression of the dominant-negative mutant dyn1(K44A) in HeLa cells that express only dyn2, potentially inhibited receptor-mediated endocytosis but had no effect on biosynthetic vesicular trafficking from the TGN to either the plasma membrane or to the lysosome (9). Therefore, in light of new evidence for dyn2 function at the TGN, it remained possible that dyn1 mutants selectively interfered with dyn2 function only at the plasma membrane.

To resolve these disparities, we compared the effects of overexpression of dominant negative mutants of dyn1 and dyn2 on membrane trafficking along both the exocytic and

endocytic pathways. We chose a splice variant of dyn2 (dyn2ba) shown to be targeted to the TGN when expressed as a GFP-fusion protein (5). We report that the effects of overexpression of the two mutant isoforms on membrane trafficking in HeLa cells were indistinguishable. Both dyn1(K44A) and dyn2(K44A) potentially inhibited receptor-mediated endocytosis of Tfn, but other membrane trafficking events were either unaffected or only slightly inhibited. These included: fluid phase endocytosis, recycling of TfnR from the endosomal compartment to the plasma membrane, transport of newly synthesized TfnR from the ER, through the Golgi and to the PM, and sorting and transport of cathepsin D at the TGN for delivery to lysosomes. In addition, overexpression of dyn2(K44A) in HeLa cells had no effect on the steady state distribution of MPR, Golgi-associated AP1 adaptors or TGN48 (see

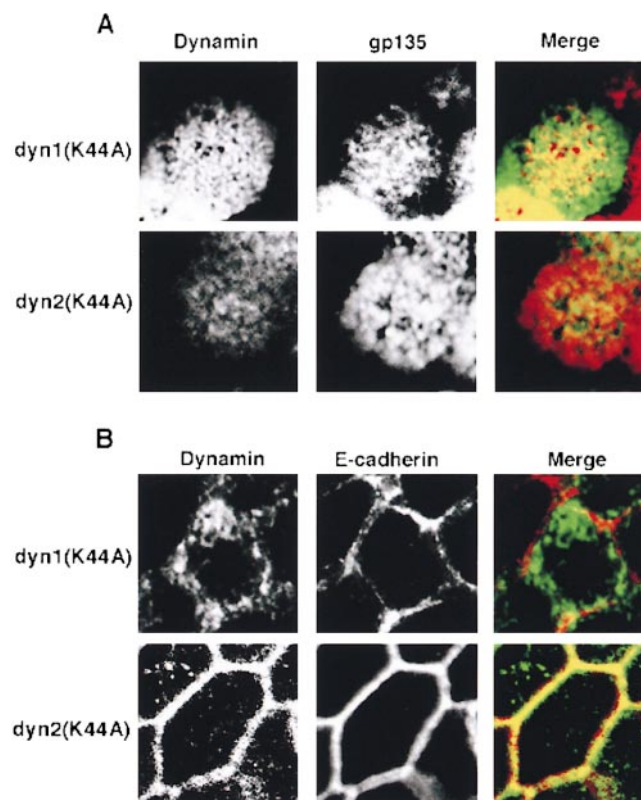


**Figure 10.** Dyn1 and dyn2 are differentially targeted to the apical and basolateral plasma membrane in polarized MDCK cells. MDCK T23 cells were infected with recombinant adenovirus encoding either HA-tagged dyn1(K44A) or dyn2(K44A), as indicated. The cells were further incubated for 18 h in the presence of 0.1 ng/ml doxycyclin (to reduce levels of overexpression) before fixation of the cells and processing for indirect immunofluorescence as described in Materials and Methods. A is a section through the apical surface, labeled with the apical plasma membrane protein, gp135, showing the targeting of dyn1(K44A) and dyn2(K44A) as detected using a rat anti-HA antibody. B is a section through a basolateral surface at the level of the nucleus showing targeting of dyn1(K44A) and dyn2(K44A) to the basolateral surface, as indicated by colocalization with E-cadherin. The excess label in the cytoplasm reflects overexpression of the recombinant dynamins.

also reference 3). Finally, we were unable to detect any colocalization of either endogenous dyn2 or overexpressed wt or mutant dyn2 with the TGN markers, TGN48 or  $\gamma$ -adaptin. In contrast, endogenous and overexpressed wt and mutant dyn2 showed extensive overlap with clathrin-coated pits at the plasma membrane. Together, these findings suggest that dyn1 and dyn2 have redundant functions when expressed in nonpolarized, nonneuronal cells and that both are selectively required for clathrin-mediated endocytosis. It is important to note that HeLa cells express very little caveolae, precluding analysis of this endocytic process in these cells.

Our suggestion that dynamin functions exclusively at the plasma membrane, is consistent with there being only a single dynamin isoform yet identified in *Drosophila* or *C. elegans*. Mutations in the *Drosophila* homologue, *shibire*, appear to specifically block endocytosis without affecting transport along the biosynthetic pathway (38). On average mammals encode four homologues of every gene in invertebrates. Although functional redundancy is common, gene duplication during evolution also allows for differential expression patterns, as exhibited by the three mammalian isoforms of dynamin. One might also expect three classes of mutations to have occurred during evolution to account for the  $\sim 20\%$  sequence divergence between the dynamin isoforms. These include: (a) mutations in nonessential residues that will not affect dynamin function; (b) mutations that enhance tissue-specific functions of the protein, such as axonal targeting and participation in regulated endocytosis in neurons; and (c) mutations that alter the posttranslational regulation of dynamin to accommodate cell-type specific regulation of endocytosis.

Identification of the functional significance of the sequence divergence between mammalian dynamin isoforms will require isoform-specific assays. To this end, we found that dyn1 and dyn2 were functionally distinguishable when expressed in polarized MDCK cells. In this case, overexpression of dyn1(K44A) more potently inhibited clathrin-mediated endocytosis at the apical surface than did dyn2(K44A), whereas the opposite was true for endocytosis at the basolateral surface. Consistent with these functional differences, dyn1 was selectively targeted to the apical surface of MDCK cells relative to dyn2. It is well established that targeting of integral membrane proteins to the apical surface of MDCK cells is analogous to targeting to the axon of neurons, and conversely that targeting to the basolateral surface of MDCK cells corresponds to the somatodendritic surface of neurons (33, 45). Our results suggest that this principle may extend to dynamin, a protein peripherally associated with the inner surface of the plasma membrane.

The apical surface of MDCK cells, like the axon, exhibits highly regulated clathrin-mediated endocytosis (33). Thus it is of interest that dyn1, when exogenously expressed in MDCK cells, apparently prefers to be involved in this regulated apical endocytosis. In contrast, endocytosis at the basolateral surface of MDCK cells resembles the relatively unregulated endocytosis found at the somatodendritic surface of neurons or the plasma membrane of fibroblasts. This unregulated endocytosis may be the normal function of dyn2. It is important to note, however, that as far as is presently known, MDCK cells do not express

dyn1 and that dyn2 is expected to act equally at both surfaces. Consistent with this, receptor-mediated endocytosis of pIgR is equally inhibited at both surfaces by overexpression of dyn2(K44A).

The inhibitory effects of overexpressed dominant-negative dynamin mutants can occur by three distinct mechanisms. First, because dynamin is a native tetramer (34), nonfunctional heterotetramers can form between wt and mutant dynamin polypeptides. Second, because dynamin self-assembly into higher order oligomers is essential for endocytosis (20, 50, 52) defective dynamin tetramers can interfere with the functional assembly of wt dynamin tetramers. Third, the overexpressed defective dynamin can ineffectively interact with other dynamin partners acting as competitive inhibitors to disrupt function. The latter two mechanisms could be isoform specific if the two isoforms are differentially targeted to their site of action or interact with different partners in the cell. The former mechanism would not be isoform-specific as long as heterotetramer formation occurs.

Our finding that dyn2 is a more potent inhibitor of endocytosis in HeLa cells than dyn1 suggests that the formation of homotetramers is preferred. However, at the levels of overexpression obtained in HeLa cells, we find that endogenous dyn2 can be quantitatively coprecipitated as a hetero-oligomer with exogenous HA-dyn1 using anti-HA antibodies (Fujimoto, M., H. Damke, and S.L. Schmid, unpublished results). This is consistent with our inability to detect differences in effects of the two mutant dynamin isoforms in HeLa cells. Moreover, based on these results we believe that the levels of overexpression in HeLa cells are sufficient to functionally interfere with all isoforms and splice variants of dynamin present. In contrast, the lower levels of overexpression obtained in MDCK cells allowed detection of the differential effects of dyn1 and dyn2 isoforms, perhaps reflecting interactions between mutant homotetramers and isoform-specific targeting or effector molecules.

In contrast to our results in HeLa cells, others have clearly established that dyn2(ba and aa) isoforms carrying a 4-aa insert can be selectively targeted to the TGN in clone 9 cells, whereas dyn2(bb and ab) isoforms lacking this insert are exclusively associated with the plasma membrane (5, 6). It is possible that neither the dyn2 splice variants carrying the insert nor the putative partner protein that selectively recognizes this insert for targeting to the TGN are expressed in HeLa cells (or presumably in MDCK cells). Our finding that dyn2 is not essential for vesicle formation from the TGN *in vivo* also conflicts with other findings suggesting (22) that dyn2 is required for the formation of both clathrin-coated and non-clathrin-coated vesicles from the TGN *in vitro*. How can these differences be reconciled? A role for dyn2 in vesicle budding from the TGN was suggested based on the loss of activity observed after multiple rounds of immunodepletion of dynamin from cytosol. Because rescue experiments were performed with only crude preparations of dynamin, it remains possible that other factor(s), nonspecifically depleted or inactivated by treatment, and present in this crude fraction were responsible for the observed restoration of vesicle budding activity. It will be important to repeat these experiments with purified dyn2. Moreover, recent experiments have

shown that dynamin can assemble into helical arrays on a number of membranes without apparent specificity in vitro (51), thus it is also possible that dynamin's participation in a vesicle budding reaction in vitro does not mirror the specificity of its function in vivo.

The function of the Golgi associated dyn2 splice variant remains to be elucidated. However, it seems unlikely, for several reasons, that dyn2 plays an essential role in vesicular trafficking from the TGN in all cells. First, we were unable to detect any localization of the endogenous dyn2 isoform with the TGN in HeLa cells. Second, we were unable to identify a TGN-based vesicular trafficking event sensitive to inhibition by dominant-negative dyn2 mutants in HeLa or MDCK cells. Third, mutations in the only dynamin isoform thus far identified in *Drosophila* do not appear to affect Golgi function (38). Fourth, recent data indicates that dyn2 is not expressed in isolated rat peripheral neurons (6). Thus, it is unlikely that dyn2 plays a universal role in vesicle budding from the TGN, as it does in endocytosis. Whether dynamin has other functions associated with the TGN or with the actin cytoskeleton (for review see reference 41) remains to be elucidated.

In this regard, it is important to consider other possibilities for the function of dynamin and dynamin-related proteins that may diverge from the better-characterized, but still unresolved, role in vesicle formation at the plasma membrane. For example, although yeast lack a true dynamin, they express two dynamin-related proteins, Vps1p and Dnm1p. Vps1p has a clear, but as yet undefined, role in vesicular trafficking between the vacuole and the Golgi (40). In contrast, recent data suggests that Dnm1p, originally implicated in endocytosis (13), instead functions by an as yet unknown mechanism in controlling mitochondrial morphology (37). Similarly, a mammalian homologue of dnm1p, originally implicated in membrane trafficking from the ER or Golgi (21, 23, 43, 62) has also been shown to function in mitochondrial structure maintenance (46). Other dynamin family members, such as the anti-viral mx proteins, are involved in even more divergent processes (47). Biochemical and functional analysis of other members of the dynamin sub-family will be needed to identify their divergent cellular functions.

We thank Dr. Kathryn Riddell-Spencer for her assistance with confocal microscopy. Several investigators generously provided antibodies and advice for their use including S. Ponnambalam, L. Traub, E. Ungewickell, S. Robinson, K. von Figura, B. Hoflack, and S. Sorokin.

This work was supported by National Institutes of Health grant GM42455 (to S.L. Schmid) and grants AI25144, AI39161, and HL55980 (to K.E. Mostov). Y. Altschuler and S.M. Barbas were supported by Postdoctoral Fellowships from the US Army Breast Cancer Program and the Juvenile Diabetes Foundation, respectively. This is TSRI manuscript no. 11849-CB.

Received for publication 18 August 1998 and in revised form 16 October 1998.

## References

1. Aroeti, B., P.A. Kosen, I.D. Kuntz, F.E. Cohen, and K.E. Mostov. 1993. Mutational and secondary structural analysis of the basolateral sorting signal of the polymeric immunoglobulin receptor. *J. Cell Biol.* 123:1149-1160.
2. Aroeti, B., and K.E. Mostov. 1994. Polarized sorting of the polymeric immunoglobulin receptor in the exocytotic and endocytotic pathways is controlled by the same amino acids. *EMBO (Eur. Mol. Biol. Organ.) J.*

- 13:2297-2304.
3. Banting, G., R. Maile, and E.P. Roquemore. 1998. The steady state distribution of humTGN46 is not significantly altered in cells defective in clathrin-mediated endocytosis. *J. Cell Sci.* 111:3451-3458.
4. Barth, A.I.M., A.L. Pollack, Y. Altschuler, K.E. Mostov, and W.J. Nelson. 1997. NH<sub>2</sub>-terminal detection of beta-catenin with adenomatous polyposis coli protein and altered MDCK cell adhesion. *J. Cell Biol.* 136:693-706.
5. Cao, H., F. Garcia, E.W. Krueger, and M.A. McNiven. 1997. Differential distribution of dynamin isoforms in mammalian cells. *Mol. Biol. Cell.* 8:424a.
6. Cao, H., F. Garcia, and M. McNiven. 1998. Differential distribution of dynamin isoforms in mammalian cells. *Mol. Biol. Cell.* 9:2595-2609.
7. Chen, M.S., R.A. Ober, C.C. Schroeder, T.W. Austin, C.A. Poodry, S.C. Wadsworth, and R.B. Vallee. 1991. Multiple forms of dynamin are encoded by *Shibire*, a *Drosophila* gene involved in endocytosis. *Nature.* 351:583-586.
8. Clark, S.G., D.L. Shurland, E.M. Meyerowitz, C.I. Bargmann, and A.M. van der Bliek. 1997. A dynamin GTPase mutation causes a rapid and reversible temperature-inducible locomotion defect in *C. elegans*. *Proc. Natl. Acad. Sci. USA.* 94:10438-10443.
9. Damke, H., T. Baba, D.E. Warnock, and S.L. Schmid. 1994. Induction of mutant dynamin specifically blocks endocytic coated vesicle formation. *J. Cell Biol.* 127:915-934.
10. Damke, H., T. Baba, A.M. van der Bliek, and S.L. Schmid. 1995. Clathrin-independent pinocytosis is induced in cells overexpressing a temperature-sensitive mutant of dynamin. *J. Cell Biol.* 131:69-80.
11. Damke, H., S. Freundlieb, M. Gossen, H. Bujard, and S.L. Schmid. 1995. Tightly regulated and inducible expression of a dominant interfering dynamin mutant in stably transformed HeLa cells. *Methods Enzymol.* 257:209-221.
12. David, C., P.S. McPherson, O. Mundigl, and P. de Camilli. 1996. A role of amphiphysin in synaptic vesicle endocytosis suggested by its binding to dynamin in nerve terminals. *Proc. Natl. Acad. Sci. USA.* 93:331-335.
13. Gammie, A.E., K.L. Kurihara, R.B. Vallee, and M.D. Rose. 1995. DNM1, a dynamin-related gene, participates in endosomal trafficking in yeast. *J. Cell Biol.* 130:553-566.
- 13a. Geiselmann, V., R. Pohmann, A. Hasilik, K. von Figura. 1993. Biosynthesis and transport of cathepsin D in cultured human fibroblasts. *J. Cell Biol.* 97:1-5.
14. Glickman, J.N., P.A. Morton, J.W. Slot, S. Kornfeld, and H.J. Geuze. 1996. The biogenesis of the MHC class II compartment in human I-cell disease B lymphoblasts. *J. Cell Biol.* 132:769-785.
15. Gossen, M., and H. Bujard. 1992. Tight control of gene expression in mammalian cells by tetracycline-responsive promoters. *Proc. Natl. Acad. Sci. USA.* 89:5547-5551.
16. Grabs, D., V.I. Slepnev, Z. Songyang, C. David, M. Lynch, L.C. Cantley, and P. De Camilli. 1997. The SH3 domain of amphiphysin binds the proline-rich domain of dynamin at a single site that defines a new SH3 binding consensus sequence. *J. Biol. Chem.* 272:13419-13425.
17. Hardy, S., M. Kitamura, T. Harris-Stansil, Y. Dai, and M.L. Phipps. 1997. Construction of adenovirus vectors through Cre-lox recombination. *J. Virol.* 71:1842-1849.
18. Henley, J.R., E.W. Krueger, B.J. Oswald, and M.A. McNiven. 1998. Dynamin-mediated internalization of caveolae. *J. Cell Biol.* 141:85-99.
19. Herskovits, J.S., C.C. Burgess, R.A. Obar, and R.B. Vallee. 1993. Effects of mutant rat dynamin on endocytosis. *J. Cell Biol.* 122:565-578.
20. Hinshaw, J.E., and S.L. Schmid. 1995. Dynamin self assembles into rings suggesting a mechanism for coated vesicle budding. *Nature.* 374:190-192.
21. Imoto, M., I. Tachibana, and R. Urrutia. 1998. Identification and functional characterization of a novel human protein highly related to the yeast dynamin-like GTPase Vps1p. *J. Cell Sci.* 111:1341-1349.
22. Jones, S.M., K.E. Howell, J.R. Henley, H. Cao, and M.A. McNiven. 1998. Role of dynamin in the formation of transport vesicles from the trans-Golgi network. *Science.* 279:573-577.
23. Kamimoto, T., Y. Nagai, H. Onogi, Y. Muro, T. Wakabayashi, and M. Hagiwara. 1998. Dymple, a novel dynamin-like high molecular weight GTPase lacking a proline-rich carboxyl-terminal domain in mammalian cells. *J. Biol. Chem.* 273:1044-1051.
24. Kessell, I., B.D. Holst, and T.F. Roth. 1989. Membranous intermediates in endocytosis are labile, as shown in a temperature-sensitive mutant. *Proc. Natl. Acad. Sci. USA.* 86:4968-4972.
25. Koenig, J.H., and K. Ikeda. 1990. Transformational process of the endosomal compartment in nephrocytes of *Drosophila melanogaster*. *Cell Tissue Res.* 262:233-244.
26. Kosaka, T., and K. Ikeda. 1983. Possible temperature-dependent blockage of synaptic vesicle recycling induced by a single gene mutation in *Drosophila*. *J. Neurobiol.* 14:207-225.
27. Kosaka, T., and K. Ikeda. 1983. Reversible blockage of membrane retrieval and endocytosis in the garland cell of the temperature-sensitive mutant of *Drosophila melanogaster*, *shibire*<sup>ts1</sup>. *J. Cell Biol.* 97:499-507.
28. Le Borgne, R., and B. Hoflack. 1997. Mannose 6-phosphate receptors regulate the formation of clathrin-coated vesicles in the TGN. *J. Cell Biol.* 137:335-345.
29. Liu, S.H., M.S. Marks, and F.M. Brodsky. 1998. A dominant-negative clathrin mutant differentially affects trafficking of molecules with distinct sort-

- ing motifs in the class II major histocompatibility complex (MHC) pathway. *J. Cell Biol.* 140:1023–1037.
30. Llorente, A., A. Rapak, S.L. Schmid, B. van Deurs, and K. Sandvig. 1998. Expression of mutant dynamin inhibits toxicity and transport of endocytosed ricin to the Golgi apparatus. *J. Cell Biol.* 140:553–563.
  31. Ludwig, T., R. Le Borgne, and B. Hoflack. 1995. Roles for mannose-6-phosphate receptors in lysosomal enzyme sorting, IGF-II binding and clathrin-coat assembly. *Trends Cell Biol.* 5:202–206.
  32. McMahon, H.T., P. Wigge, and C. Smith. 1997. Clathrin interacts specifically with amphiphysin and is displaced by dynamin. *FEBS Lett.* 413:319–322.
  33. Mostov, K.E., and M.H. Cardone. 1995. Regulation of protein traffick in polarized epithelial cells. *Bioessays.* 17:729–738.
  34. Muhlberg, A.B., D.E. Warnock, and S.L. Schmid. 1997. Domain structure and intramolecular regulation of dynamin GTPase. *EMBO (Eur. Mol. Biol. Organ.) J.* 16:6676–6683.
  35. Oh, P., D.P. McIntosh, and J.E. Schnitzer. 1998. Dynamin at the neck of caveolae mediates their budding to form transport vesicles by GTP-driven fission from the plasma membrane of endothelium. *J. Cell Biol.* 141:101–114.
  36. Okamoto, P.M., J.S. Herskovits, and R.B. Vallee. 1997. Role of the basic, proline-rich region of dynamin in Src homology 3 domain binding and endocytosis. *J. Biol. Chem.* 272:11629–11635.
  37. Otsuga, D., B.R. Keegan, G.J. Hermann, E. Brisch, W. Bleazard, and J.M. Shaw. 1998. The dynamin-like GTPase, Dnm1p, controls mitochondrial morphology in yeast. *J. Cell Biol.* 143:333–349.
  38. Radhakrishna, H., R.E. Pagano, C.E. Machamer, and T.F. Roth. 1993. Endocytosis is not required for the exocytosis of VSV-G protein or C<sub>6</sub>-NBD sphingolipids to the plasma membrane in *shibire* cells. *Mol. Biol. Cell.* 4:211a.
  39. Roos, J., and R. Kelly. 1997. Is dynamin really a “pinchase”. *Trends Cell Biol.* 7:257–259.
  40. Rothman, J.H., C.K. Raymond, T. Gilbert, P.J. O’Hara, and T.H. Stevens. 1990. A putative GTP binding protein homologous to interferon-inducible Mx proteins performs an essential function in yeast protein sorting. *Cell.* 61:1063–1074.
  41. Schmid, S., M. McNiven, and P. De Camilli. 1998. Dynamin and its partners: A progress report. *Curr. Opin. Cell Biol.* 10:504–512.
  42. Seeger, M., and G.S. Payne. 1992. Selective and immediate effects of clathrin heavy chain mutations on Golgi membrane protein retention in *Saccharomyces cerevisiae*. *J. Cell Biol.* 118:531–540.
  43. Shin, H.W., C. Shinotsuka, S. Torii, K. Murakami, and K. Nakayama. 1997. Identification and subcellular localization of a novel mammalian dynamin-related protein homologous to yeast Vps1p and Dnm1p. *J. Biochem.* 122:525–530.
  44. Shpetner, H.S., J.S. Herskovits, and R.B. Vallee. 1996. A binding site for SH3 domain targets dynamin to coated pits. *J. Biol. Chem.* 271:13–16.
  45. Simons, K., P. Dupree, K. Fiedler, L.A. Huber, T. Kobayashi, T. Kurzchalia, V. Olkkonen, S. Pimplikar, R. Parton, and C. Dotti. 1992. Biogenesis of cell-surface polarity in epithelial cells and neurons. *Cold Spring Harb. Symp. Quant. Biol.* 57:611–619.
  46. Smirnova, E., D.-L. Shurland, S.N. Ryazantsev, and A.M. van der Blik. 1998. A human dynamin-related protein controls the distribution of mitochondria. *J. Cell Biol.* 143:351–358.
  47. Staeheli, P., F. Pitossi, and J. Pavlovic. 1993. Mx proteins: GTPases with antiviral activity. *Trends Cell Biol.* 3:268–272.
  48. Stoorvogel, W., V. Oorschot, and H.J. Geuze. 1996. A novel class of clathrin-coated vesicles budding from endosomes. *J. Cell Biol.* 132:21–33.
  49. Sweitzer, S., and J. Hinshaw. 1998. Dynamin undergoes a GTP-dependent conformational change causing vesiculation. *Cell.* 93:1021–1029.
  50. Takei, K., P.S. McPherson, S.L. Schmid, and P. De Camilli. 1995. Tubular membrane invaginations coated by dynamin rings are induced by GTPγS in nerve terminals. *Nature.* 374:186–190.
  51. Takei, K., V. Haucke, V. Slepnev, K. Farsad, M. Salazar, H. Chen, and P. De Camilli. 1998. Generation of coated intermediates of clathrin-mediated endocytosis on protein-free liposomes. *Cell.* 94:131–141.
  52. Tuma, P.L., and C.A. Collins. 1995. Dynamin forms polymeric complexes in the presence of lipid vesicles. Characterization of chemically cross linked dynamin molecules. *J. Biol. Chem.* 270:26707–26714.
  53. Urrutia, R., J.R. Henley, T. Cook, and M.A. McNiven. 1997. The dynamins: redundant or distinct functions for an expanding family of related GTPases? *Proc. Natl. Acad. Sci. USA.* 94:377–384.
  54. van der Blik, A.M., and E.M. Meyerowitz. 1991. Dynamin like protein encoded by the *Drosophila shibire* gene associated with vesicular traffic. *Nature.* 351:411–414.
  55. van der Blik, A.M., T.E. Redelmeier, H. Damke, E.J. Tisdale, E.M. Meyerowitz, and S.L. Schmid. 1993. Mutations in human dynamin block an intermediate stage in coated vesicle formation. *J. Cell Biol.* 122:553–563.
  56. Wang, L.H., T.C. Sudhof, and R.G. Anderson. 1995. The appendage domain of alpha adaptin is a high affinity binding site for dynamin. *J. Biol. Chem.* 270:10079–10083.
  57. Warnock, D.E., and S.L. Schmid. 1996. Dynamin GTPase, a force generating molecular switch. *Bioessays.* 18:885–893.
  58. Warnock, D.E., L.J. Terlecky, and S.L. Schmid. 1995. Dynamin GTPase is stimulated by crosslinking through the C terminal proline rich domain. *EMBO (Eur. Mol. Biol. Organ.) J.* 14:1322–1328.
  59. Warnock, D.E., T. Baba, and S.L. Schmid. 1997. Ubiquitously expressed dynamin-II has a higher intrinsic GTPase activity and a greater propensity for self-assembly than neuronal dynamin-I. *Mol. Biol. Cell.* 8:2553–2562.
  60. Wigge, P., K. Kohler, Y. Vallis, C.A. Doyle, D. Owen, S.P. Hunt, and H.T. McMahon. 1997. Amphiphysin heterodimers: potential role in clathrin-mediated endocytosis. *Mol. Biol. Cell.* 8:2003–2015.
  61. Wigge, P., Y. Vallis, and H.T. McMahon. 1997. Inhibition of receptor-mediated endocytosis by the amphiphysin SH3 domain. *Curr. Biol.* 7:554–560.
  62. Yoon, Y., K.R. Pitts, S. Dahan, and M.A. McNiven. 1998. A novel dynamin-like protein associates with cytoplasmic vesicles and tubules of the endoplasmic reticulum in mammalian cells. *J. Cell Biol.* 140:779–793.